

High-repetition-rate femtosecond optical parametric oscillator based on periodically poled lithium niobate

Kent C. Burr^{a)} and C. L. Tang
Cornell University, Ithaca, New York 14853

Mark A. Arbore and Martin M. Fejer
Stanford University, Stanford, California 94305

(Received 19 February 1997; accepted for publication 23 April 1997)

A high-repetition-rate, femtosecond optical parametric oscillator based on bulk periodically poled lithium niobate is described. This optical parametric oscillator is continuously tunable from 1.12 to 1.50 μm in the signal branch, and signal pulses as short as 60 fs have been observed. The corresponding tuning range for the idler branch is from 1.68 to 2.72 μm . Modifications which should result in a femtosecond optical parametric oscillator with a pumping threshold of less than 50 mW are discussed. © 1997 American Institute of Physics. [S0003-6951(97)04325-8]

Periodically poled lithium niobate (PPLN) has emerged as an important nonlinear material for use in optical parametric oscillators¹ (OPOs). PPLN OPO's have been demonstrated in the cw,² nanosecond,^{3,4} and picosecond^{5,6} regimes. Pulsed parametric superluminescence on the order of 300 fs, at a repetition rate of 1–10 kHz, was also recently observed in PPLN.⁷ This letter reports what we believe is the first demonstration of a high-repetition-rate, femtosecond OPO based on PPLN or any other quasi-phase-matched material. Using a femtosecond Ti:sapphire laser to synchronously pump the PPLN OPO, the signal branch was continuously tunable from 1.12 to 1.50 μm , and signal pulses as short as 60 fs were observed. The corresponding idler tuning range was 1.68–2.72 μm , and the potential tuning range extends to beyond 5 μm . With improvements to the OPO described in this letter, threshold pumping levels below 50 mW should be readily accessible. The potential tuning range and extremely low threshold level should make PPLN an important crystal for use in all-solid-state broadly tunable femtosecond sources.

The quasi-phase-matching⁸ (QPM) condition employed with PPLN allows the coupling of interacting waves through the largest element of the $\chi^{(2)}$ tensor. Since d_{33} is an order of magnitude larger than the other nonlinear coefficients of lithium niobate, polarizing all three waves along the z axis ($e \rightarrow e + e$) results in the highest effective nonlinearity. This coefficient cannot be accessed through birefringent phase matching. In comparison with other nonlinear materials such as KTiOPO_4 (KTP) and LiB_3O_5 (LBO), which are commonly used for femtosecond OPO's, PPLN has a much larger effective nonlinear coefficient, but its group velocity mismatch (GVM) between the interacting waves is also larger. The GVM results in a limited effective interaction length. The nonlinear coefficient and GVM can be combined in a material figure of merit (FOM)^{6,9} for ultrashort nonlinear interactions which can be used to compare the theoretical efficiencies of different nonlinear materials. To estimate the FOM for an OPO operating in the above mentioned wavelength range, one can consider a degenerate interaction in which the signal and idler wavelengths are equal. Calculations, such as

those presented in Ref. 9 with a pump wavelength of $\lambda_P = 0.780 \mu\text{m}$ and signal and idler wavelengths of $\lambda_S = \lambda_I = 1.56 \mu\text{m}$, show that PPLN has a FOM that is approximately an order of magnitude larger than that of KTP or LBO. The FOM of KNbO_3 is closer to that of PPLN.

The PPLN crystal used in this experiment had a grating period of $\Lambda = 19.5 \mu\text{m}$ and was 800 μm long. Both sides of the crystal were coated with a single layer of MgF_2 to reduce the reflection losses, which are $>13\%$ per surface at our signal wavelength range for an uncoated crystal. Unfortunately, the thickness of the coating was not ideal for our wavelength range, resulting in reflection losses of $\sim 7\%$ per surface for the signal and $\sim 11\%$ per surface for the pump. Nevertheless, the PPLN OPO oscillated robustly, and better anti-reflection coating will improve the results.

Although using a collinear geometry and tuning the crystal temperature allows for noncritical phase matching, we used a geometry with a small noncollinear angle between the pump and signal (see Fig. 1) for two reasons. First, a collinear geometry requires the use of expensive optics which must be highly transmissive for the pump and highly reflective for the signal. Such optics were not readily available in our laboratory at the time the experiment was performed. Second, using a small noncollinear angle makes for easy collection of the idler and residual pump beam, which exit the crystal at different angles and can be picked off with separate mirrors. We used a noncollinear angle of $\sim 2.5^\circ$ (measured external to the crystal) in the plane of polarization of the pump and signal. The focusing parameters of the cavity were chosen so that the small noncollinear angle did not significantly limit the interaction length in the crystal.

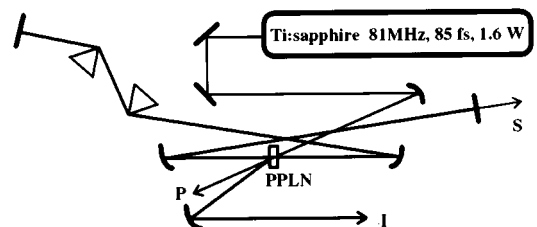


FIG. 1. Schematic of the femtosecond PPLN OPO. The cavity and crystal are aligned so that the Ti:sapphire pump (P), signal (S), and idler (I) are all e -waves, polarized in the plane of the figure.

^{a)}Electronic mail: kb12@cornell.edu

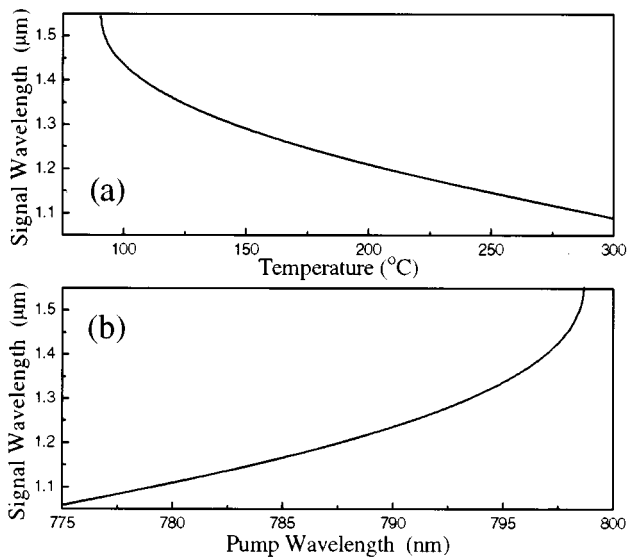


FIG. 2. Calculated signal tuning curves for PPLN OPO with a quasi-phase-matching period of $19.5\mu\text{m}$ and an external noncollinear angle of 2.5° between the pump and signal: (a) temperature tuning with a pump wavelength of 793 nm and (b) pump tuning at a temperature of 150°C .

The Ti:sapphire pump laser had a central wavelength of 793 nm , and it produced 85 fs , nearly transform-limited pulses. The repetition rate was 81 MHz , and the average pump power was 1.60 W . The pump beam was focused into the PPLN crystal by an $r=30\text{ cm}$ mirror. The linear OPO cavity consisted of two $r=15\text{ cm}$ mirrors and a flat mirror, all coated for high reflectivity between 1.1 and $1.5\mu\text{m}$. Three different output couplers were used with transmission varying from $\sim 1\%$ to $\sim 9\%$ over the tuning range of the OPO. The intracavity dispersion compensating prism sequence consisted of two SF14 prisms spaced at 22 cm . The idler was collected and collimated with an $r=20\text{ cm}$ silver mirror.

The crystal was mounted on a copper block and always maintained at a temperature $>75^\circ\text{C}$ to avoid photorefractive damage.³ The copper block was heated by a cartridge heater (OMEGA model No. CIR-1013/120), and the temperature was measured with a thermocouple mounted next to the crystal on the copper block. Feedback control for the heater was found to be unnecessary. The ability to control the crystal temperature also allowed us to temperature tune the signal wavelength. Calculated tuning curves, based on the Sellmeier equations given in Ref. 10, for temperature tuning and pump tuning are shown in Fig. 2.

The OPO produced as much as 155 mW average power in the signal beam measured directly outside the output coupler, but we estimate that including reflection losses from the crystal surfaces as much as 360 mW was generated in the signal branch. In the idler branch, which saw less than 1% loss at the crystal surface, we measured 265 mW . Significant power was also generated in the sum-frequency of the signal and Ti:sapphire. Due to geometrical constraints, we were not able to directly measure the power in this beam, but based on the measured pump depletion we estimate that, for certain crystal temperatures and signal wavelengths, on the order of 200 mW was generated at the sum-frequency wavelength ($\sim 460\text{--}520\text{ nm}$). It should be noted that the maximum

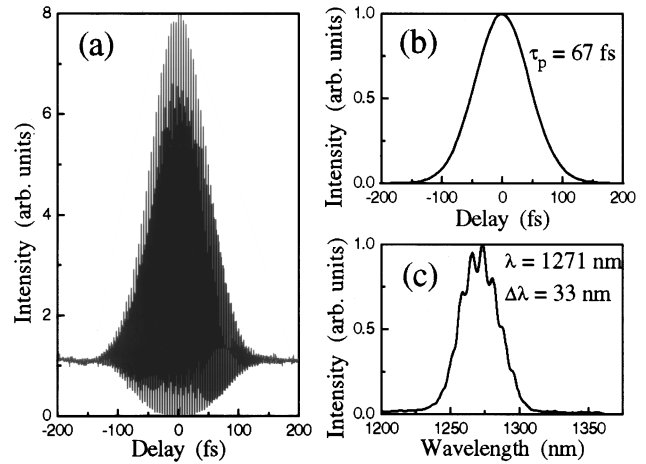


FIG. 3. (a) Interferometric and (b) intensity autocorrelation traces and (c) the corresponding spectrum for signal pulses from the PPLN OPO.

power in all beams did not occur simultaneously.

Pulse durations were measured with a collinear autocorrelator. For the signal beam a $300\text{-}\mu\text{m}$ -thick piece of β -barium borate was used to generate second harmonic which was detected by a photomultiplier tube. The idler autocorrelations were measured by two-photon absorption in a photodiode.¹¹ Pulse durations as short as 60 fs were measured for the signal branch, assuming a sech^2 intensity profile. Figure 3 shows interferometric and intensity autocorrelations and a spectrum for typical signal pulses. The time-bandwidth product for these pulses was $\Delta\nu\Delta\tau=0.41$, indicating along with the interferometric autocorrelation that the pulses are close to the transform limit. The slight modulation on the spectrum was caused by an étalon effect in a thin beamsplitter placed in the beam outside the cavity. We have verified that this beamsplitter had a negligible effect on the measured pulsewidths and bandwidths. For the idler branch, which did not include any dispersion compensating elements, we typically measured pulsewidths of $\sim 100\text{ fs}$.

The tuning range of the signal branch was $1.12\text{--}1.50\mu\text{m}$, corresponding to a tuning range of $1.68\text{--}2.72\mu\text{m}$ for the idler branch. The tuning range of the signal was limited by the reflectivity of the cavity mirrors. Attenuation coefficient data⁴ for lithium niobate suggests that the tuning range of the femtosecond PPLN OPO could be extended significantly further into the infrared, possibly rivaling the KNbO_3 OPO¹² for generation of tunable femtosecond pulses at wavelengths near $5\mu\text{m}$. Tuning was accomplished by a combination of length tuning¹³ and temperature tuning. Because the tuning curve as a function of pump wavelength is relatively steep and the pump beam had a bandwidth of more than 8 nm , at a given crystal temperature we were able to tune over $\sim 150\text{ nm}$ by changing the cavity length. Adjusting the temperature along with the cavity length resulted in improved efficiency over the entire tuning range. To achieve near transform-limited pulses, the intracavity dispersion also had to be adjusted as the wavelength was tuned. The effect of changing the cavity length while keeping the crystal temperature and intracavity dispersion compensation constant is shown in Fig. 4. As the length is reduced from a length which produces short, nearly transform-limited pulses, the OPO oscillates at two distinct wavelengths, sometimes sepa-

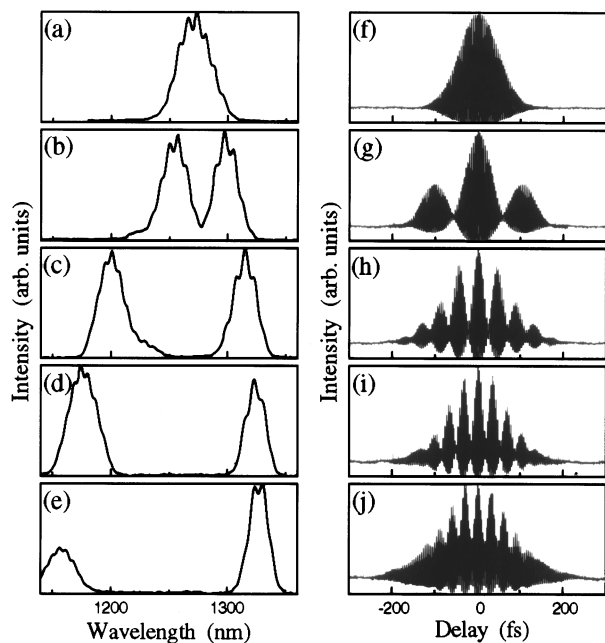


FIG. 4. Effect of cavity length changes on OPO operation: (a) shows the OPO signal spectrum when the cavity length is optimized for short pulse-width. (b)–(e) show the signal spectrum as the cavity length is continuously decreased. (f)–(j) show the corresponding interferometric autocorrelation traces.

rated by as much as 150 nm. The beat patterns in the interferometric autocorrelations demonstrate that the OPO is truly oscillating at two wavelengths simultaneously. Similar bichromatic emission has been observed in other femtosecond OPO systems¹⁴ and in femtosecond Ti:sapphire lasers,¹⁵ and it is explained in Ref. 14. The total change in cavity length for the data shown in Fig. 4 is $\sim 6 \mu\text{m}$. The spectra were recorded simultaneously with the interferometric autocorrelations using a laser spectrum analyzer scanning at 30 Hz. Again, the modulation on the spectra was caused by an étalon effect in a thin beamsplitter.

After replacing the output coupler with a high reflector for the signal wavelength, which gave us a cavity that still had substantial round-trip loss due to reflections from the crystal, we measured a pump power threshold of 580 mW incident on the PPLN crystal. By replacing our PPLN crystal with a properly coated crystal or a brewster-cut crystal, which would greatly reduce reflection losses for both the signal and the pump, and by using a ring cavity to further reduce loss, the total round-trip loss could be reduced from an estimated 26% with the high reflector to $\sim 2.5\%$, while allowing for significant useful outcoupling. Such a reduction in round-trip loss would result in a threshold¹ of less than 50 mW of pump power (measured internal to the crystal) for the crystal length used in this experiment. This predicted threshold level is much lower than thresholds for other synchronously pumped femtosecond OPO's, which are typically in the range of several hundred milliwatts. Further threshold reduction could be achieved by using a collinear geometry

which would allow for much tighter focusing without reducing the interaction length. The extremely low threshold pumping level means that the PPLN OPO could be incorporated into a all-solid-state system consisting of a mode-locked Ti:sapphire laser powered by a commercially available frequency-doubled diode-pumped laser to produce tunable femtosecond pulses in the near- to mid-infrared. Alternatively, with a brewster-cut or properly coated PPLN crystal, the crystal length could be reduced greatly, resulting in lower dispersion, and allowing one to take advantage of the large bandwidth to produce extremely short, tunable, infrared pulses.

In summary, we have demonstrated the operation of a femtosecond high-repetition-rate PPLN OPO. The OPO signal was continuously tunable from 1.12 to 1.50 μm , and chirp-free signal pulses as short as 60 fs were generated. The corresponding tuning range for the idler was 1.68–2.72 μm , with pulsewidths of ~ 100 fs, and as much as 265 mW of average power. The potential tuning range for the idler extends to beyond 5 μm . By reducing reflection losses from the crystal surface, we estimate that the threshold pumping level of the femtosecond PPLN OPO could be reduced to less than 50 mW.

Note added in proof: We have recently demonstrated all-solid-state pumping of the femtosecond PPLN OPO, and we have extended the turning range to 5.4 μm . These results will be presented in a future publication.

The authors thank P. E. Powers and F. Ganikhanov for helpful conversations. This research was supported by the Joint Services Electronics Program and the National Science Foundation.

¹ See for example, C. L. Tang and L. K. Cheng, *Fundamentals of Optical Parametric Processes and Oscillators* (Harwood Academic, Amsterdam, 1995).

² W. R. Bosenberg, A. Drobshoff, J. I. Alexander, L. E. Myers, and R. L. Byer, *Opt. Lett.* **21**, 1336 (1996).

³ L. E. Myers, R. C. Eckardt, M. M. Fejer, R. L. Byer, W. R. Bosenberg, and J. W. Pierce, *J. Opt. Soc. Am. B* **12**, 2101 (1995).

⁴ L. E. Myers, R. C. Eckardt, M. M. Fejer, R. L. Byer, and W. R. Bosenberg, *Opt. Lett.* **21**, 591 (1996).

⁵ S. D. Butterworth, V. Pruneri, and D. C. Hanna, *Opt. Lett.* **21**, 1345 (1996).

⁶ V. Pruneri, S. D. Butterworth, and D. C. Hanna, *Appl. Phys. Lett.* **69**, 1029 (1996).

⁷ A. Galvanauskas, M. A. Arbore, M. M. Fejer, M. E. Fermann, and D. Harter, *Opt. Lett.* **22**, 105 (1997).

⁸ M. M. Fejer, G. A. Magel, D. H. Jundt, and R. L. Byer, *IEEE J. Quantum Electron.* **28**, 2631 (1992).

⁹ M. A. Arbore, M. M. Fejer, M. E. Fermann, A. Hariharan, A. Galvanauskas, and D. Harter, *Opt. Lett.* **22**, 13 (1997).

¹⁰ G. J. Edwards and M. Lawrence, *Opt. Quantum Electron.* **16**, 373 (1984).

¹¹ Y. Takagi, T. Kobayashi, K. Yoshihara, and S. Imamura, *Opt. Lett.* **17**, 658 (1992).

¹² D. E. Spence, S. Wielandy, C. L. Tang, C. Bosshard, and P. Günter, *Appl. Phys. Lett.* **68**, 452 (1996).

¹³ D. C. Edelstein, E. S. Wachman, and C. L. Tang, *Appl. Phys. Lett.* **54**, 1728 (1989).

¹⁴ T. J. Driscoll, G. M. Gale, and F. Hache, *Opt. Commun.* **110**, 638 (1994).

¹⁵ M. R. X. de Barros and P. C. Becker, *Opt. Lett.* **18**, 631 (1993).